DOI: 10.21062/mft.2022.073 http://www.journalmt.com

The Influence of Fe Content on Corrosion Resistance of secondary AlSi7Mg0.3 Cast Alloy with Increased Fe-content

Zuzana Šurdová (0000-0002-4823-2279), Lenka Kuchariková (0000-0002-2688-1075), Eva Tillová (0000-0002-1010-0713), Lucia Pastierovičová (0000-0001-5341-9292), Mária Chalupová (0000-0003-0175-9484), Milan Uhríčik (0000-0002-2782-5876), Martin Mikolajčík (0000-0002-7477-6237)
Faculty of Mechanical Engineering, Department of Materials Engineering, University of Žilina, Univerzitná 8215/1, 010 26 Žilina. Slovakia. E-mail: zuzana.surdova@fstroj.uniza.sk

Production of primary aluminium is energetically enormously expensive. The use of secondary (recycled) aluminium, has therefore a high potential to save money and energy while reducing the negative environmental impact of aluminium production. Although the properties of secondary aluminium alloys are generally comparable to those of primary aluminium alloys, the increased Fe content can lead to a significant reduction in the corrosion resistance of these alloys. Secondary (recycled) AlSi7Mg0.3 cast alloy with different iron contents (0.123, 0.454, 0.679 and 1.209 wt. %) in the as-cast and after heat treatment (T6) condition was investigated. The quantitative analysis was focused on the evaluation of the Fe-phases, especially the needle-like Al_5FeSi phase. The corrosion resistance was measured by a rapid corrosion test (AUDI test). The corrosion damage of the surface was observed macroscopically. The results show that Fe content higher than 0.454 % has no significant effect on the amount and size of needle-like phases of Al_5FeSi. The corrosion resistance is mainly influenced by the size and length of the Al_5FeSi phases. Increased Fe content decreases the corrosion resistance of AlSi7Mg0.3 alloy and accelerates the initiation of corrosion.

Keywords: AlSi7Mg0.3 cast alloy, Fe-phase, corrosion resistance, AUDI test

1 Introduction

Aluminium is one of the most used metals in the modern world. The main reason is a good combination of properties (lightweight, corrosion resistance, castability and machinability) of aluminium-based alloys. The downside of using primary aluminium is the manufacturing price, because of the amount of energy used in its production. Secondary aluminium gets its name from its source. It is 'secondary' because it is made from recycled aluminium scrap. This scrap can come from all sorts of aluminium products and profiles, such as aluminium turnings, aluminium sheets, aluminium shreds, aluminium radiators, cast aluminium, extrusions, painted sidings, aluminium dross, and more. The most laborious aspect of secondary aluminium production is the cleaning and separation of aluminium scrap from other materials. After processing, it is smelted, usually using natural gas. The energy requirements for secondary production are therefore much less energy intensive compared to primary aluminium. The statistics bear this out – an increase in the aluminium recycling rate of just 10 % can reduce gas emissions from aluminium processing by up to 15 % and recycling aluminium scraps requires 95 % less energy than primary production. Generally, secondary aluminium has a higher tolerance for alloying elements, such as iron, magnesium, and silicon (which are commonly added in the recycling process) [1-4].

Al-Si-based alloys are the most used aluminium casting alloys. On the surface of said alloys, a barrier oxide film that is strongly bonded to its surface is formed as soon as being in contact with air. This oxide film is the most stable in aqueous media with a pH between 4.0 and 8.5. If this barrier is damaged (e.g., by open-air solutions containing halide ions) it re-forms immediately in most environments. The surface of cast Al-Si-Mg alloys contains not only aluminium oxide but also mixed Al-Mg oxide [5-7].

AlSi7Mg0.3 cast alloy is an aluminium alloy that is characterized by good casting properties, good corrosion resistance and machinability. The most common type of corrosion attacking AlSi7Mg0.3 alloy is pitting corrosion. This type of corrosion is localized and usually manifested by random pitting. Only a small part of the surface is attacked, but the corrosion progresses intensively in depth. Once initiated, this type of corrosion is very unpredictable [7-9].

This paper focuses on secondary AlSi7Mg0.3 cast alloy with increased iron content. This may be caused by iron introduced into the AlSi7Mg0.3 alloy during melting from scrap, through the melting medium or the handling equipment used. The high iron content of secondary aluminium alloys is therefore a serious

problem because it is impossible to eliminate its negative effect. Since iron has low solubility in aluminium alloys, it is precipitated in the form of intermetallic phases. The intermetallic phases are, for example, needle/plate-like Al_5FeSi, plate-like Al_6Fe or Al_5Fe. Mn-alloyed alloys contain the skeleton-like or Chinese script-shaped $Al_{15}FeMn_3Si_2$ phase. Hard and brittle Al_5FeSi platelets/needles have a detrimental influence on the properties of the alloy. These phases cause porosity, lower fluidity, act as stress concentrators, promote crack initiation, and reduce impact strength, machinability, and fatigue life. From the electrochemical point of view, the Al_5FeSi phase is nobler than the matrix in aqueous media, making the alloy system highly susceptible to localised corrosion. The higher content of Fe causes an increase in forming of a long and higher amount of Fe needle phases as a decrease in ductility and corrosion properties, too [9-15]. Many studies show that the effect of Fe-rich phases on the corrosion resistance and the mechanical or fatigue properties of aluminium alloys depends on their type, size, and amount. The major problem can occur once the critical value of the iron content is exceeded, which is individual for each alloy and depends on the silicon content of the aluminium alloy. The critical iron content of the AlSi7Mg0.3 alloy, which is the subject of this paper, is approximately 0.5 % [9-15].

Magnesium, present in the microstructure of Al-Si-Mg alloys can form intermetallic phases such as Mg_2Si, $Al_8FeMg_3Si_6$ or $Al_9FeMg_3Si_5$. These phases can cause improved corrosion resistance, along with weldability, work-hardening and strengthening. The studies show that as little as 1 wt. % of added magnesium causes a reduction in the size of pits caused by pitting corrosion. After the addition of 4.5 - 9 wt. % Mg, the pits and pitting marks disappear completely from the surface of Al-Si alloys [14, 16-17].

In the current practice, there are several ways of the corrosion resistance testing of aluminium alloys. Exposure methods such as immersion tests and corrosion resistance tests in the condensing chamber are carried out in various corrosion environments, depending on the application of said alloys. Another type of corrosion testing method is the electrochemical method. These include for example potentiodynamic and potentiostatic tests, electrochemical impedance spectroscopy and others [7, 15, 18-19].

Al-Si-Mg alloys in general are widely used in the automotive, aerospace and even food industry. Good castability and corrosion resistance makes these alloys suitable for automotive applications such as engine brackets and mufflers. However, it is particularly important that the alloy has good thermal conductivity, because these components could get overheated. Other areas of use are for example shipbuilding (anchors), the aerospace industry, in favour of reducing the weight of the plane (wing skins, fuelling fittings, overwing emergency door exit) and the chemical industry [20-22].

The paper aims to study the effect of Fe on the morphology and number of Fe-rich intermetallic phases and to evaluate the corrosion resistance using the rapid AUDI test. The work is part of the VEGA 01/0398/19 project focused on the study of secondary alloys with higher iron content.

2 Materials and methods

Investigated samples of secondary AlSi7Mg0,3 aluminium cast alloy were produced at UNEKO, spol. s.r.o, Zátor, Czech Republic and they were supplied in a form of circular rods with 20 mm diameter and length of 300 mm. All the samples were made by gravity casting into sand moulds (Fig. 1). These moulds have been treated with a protective spray that prevents penetration of liquid metal into the sand mould and thus ensures a better-quality surface.

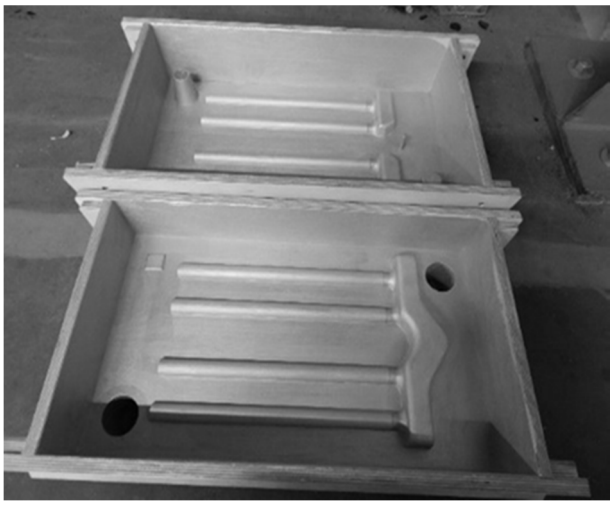

Fig. 1 *Moulds used for sand casting*

To evaluate the effect of higher Fe content on the presence of Fe-rich intermetallic phases and the corrosion resistance, 4 melts were cast with different iron contents in wt.%: 0.123 (alloy A); 0.454 (alloy B); 0.679 (alloy C) and 1.209 (alloy D). The chemical composition of investigated aluminium alloys and the calculated critical iron value are shown in Tab. 1. The casting temperature for each melt was 750 °C and the refining temperature was 740 - 745 °C. From each melt, 24 bars were cast, and half of the bars were subjected to heat treatment T6. These samples were compared to determine whether the heat treatment improves corrosion resistance and lowers the amount of Fe-rich intermetallic phases in needle forms present in the microstructure.

Tab. 1 *Chemical composition of experimental AlSi7Mg0.3 cast alloy (wt. %)*

Alloy	Si	Fe	Cu	Mn	Mg	Cr	Zn	Ti	Ga	V	Al	$Fe_{crit.}$
A	7.028	0.123	0.013	0.01	0.35	0.002	0.04	0.12	0.01	0.01	ball.	0.48
B	7.340	0.454	0.021	0.01	0.3	0.002	0.02	0.12	0.01	0.01	ball.	0.50
C	7.346	0.679	0.0096	0.01	0.4	0.002	0.03	0.11	0.01	0.01	ball.	0.50
D	7.340	1.209	0.01	0.01	0.31	0.002	0.01	0.12	0.01	0.01	ball.	0.50

Microstructure analysis has been done to determine the connection between microstructure and corrosion resistance as well as the influence of heat treatment on investigated AlSi7Mg0.3 alloys. The experimental samples have been prepared using a suitable metallographic procedure, consisting of grinding with 500 and 1 200 - grit Strues SiC grinding paper, followed by polishing with 3 μm diamond paste and Strues Op-S. The etcher 0.5 % HF and H_2SO_4 were used for chemical etching, the latter, to highlight Fe-rich phases in the microstructure of investigated alloys. Prepared samples were observed by optical microscope NEOPHOT 32.

Quantitative analysis of Fe-rich phases was performed using an optical microscope with NIS Elements 5.2 software. This was done to evaluate the effect of the Fe content and heat treatment on the length of Fe-rich phases, focusing mainly on the phases in the plate-like (needle) form. The length of Fe-rich intermetallic phases in needle form was measured 50 times on all the experimental samples, with and without heat treatment (T6).

The corrosion resistance of investigated samples from secondary AlSi7Mg0.3 alloy was examined. AUDI test, an internal PV 11 13 standard for the automotive industry, was chosen to evaluate the corrosion behaviour of these samples [23]. The specimens used for this test were 18 mm in diameter and 10 mm long, and for each melt, 3 specimens were used for this test. Before testing each specimen was degreased in ethanol and dried with hot air. Then all the specimens were weighed using analytical scales with an accuracy of 5 to 6 decimal places and immersed in AUDI solution – 1 dm^3 H_2O + 20 g NaCl + 0,1 dm^3 20 % HCl for 2 hours at 20 ± 2 °C. After the test, each specimen was rinsed in distilled water and ethanol, dried with hot air and weighed. Afterwards, the specimens were visually evaluated using Olympus Stereo microscope SZX16, to determine the influence of increased Fe content and heat treatment on the investigated alloy.

3 Results and discussion

3.1 Structural analysis

Typical microstructures of the experimental alloys are shown in Fig. 2. The microstructure consists of α-phase, eutectic (dark grey crystals Si in α- phase) and various types of intermetallic phases. The α-matrix crystallises from the liquid as the primary phase in the form of dendrites. Silicon is observed in alloys in the cast state in the shape of more angular grains and after heat treatment as fine round particles. The intermetallic phases identified were Fe-rich (Al_5FeSi needles) and Mg-rich (Mg_2Si very fine particles).

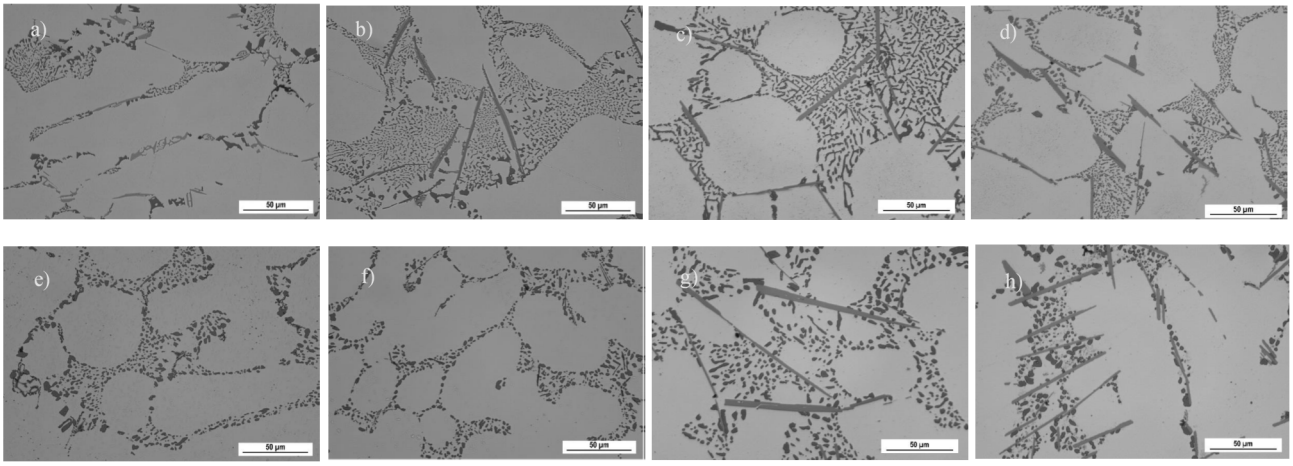

Fig. 2 *Microstructure of experimental alloys with different amount of Fe, in as-cast state – a) 0.123 Fe; b) 0.454 Fe, c) 0.679 % Fe and d) 1.209 Fe; after T6 - e) 0.123 Fe; f) 0.454 Fe, g) 0.679 Fe and h) 1.209 Fe; etch. 0.5 % HF*

The results of the metallographic observation carried out showed that as the iron content increased, the presence of the needle-like Al_5FeSi phase increased in the alloys. An increase in their length, as well as thickness, was also observed. The same tendency of Fe's on Al_5FeSi phases influence was also seen in the melts

after heat treatment. Heat treatment preferentially affects the spheroidization of eutectic silicon. The melts with heat treatment led to significant spheroidization of the eutectic silicon, but its size was strongly influenced by the amount of Fe needle-like phases in the microstructure. The effect of the T6 on the intermetallic phases was manifested in the fragmentation of the Fe intermetallic phases into smaller formations and the dissolution of the Mg_2Si phase in the matrix [24-25].

3.2 Quantitative analysis

The results of the quantitative analysis are documented in Tab. 2 and Fig. 3 and 4. The results show that an increase in Fe content does not necessarily lead to an increase in the average length of the Fe phases and the length of the Al_5FeSi needles is mainly affected by the heat treatment when the so-called phase segmentation occurs. The shortest average length of the intermetallic phase of Al_5FeSi in alloys without heat treatment was observed in alloy A with a minimum iron content (0.123 % Fe), which corresponds to the chemical composition of the primary alloy. In the alloys with increasing Fe content, a constant increase in the average length of the Al_5FeSi phases was not observed. The average length of needle-like phases was less in alloys D and C than in alloy B, probably due to the same critical iron value ($Fe_{crit.}$ - 0.5 - Tab. 1).

If we compare alloys with the same % Fe without and after heat treatment (Tab. 2), it can be concluded that after T6 heat treatment, a decrease (reduction) in the average needle length was observed in alloys with an iron content of up to 1.209 % Fe. This reduction decreased with increasing iron content from 51 % for alloy A to 15 % for alloy D.

Tab. 2 *The results of quantitative analysis of Fe intermetallic phases in form of needles*

Alloy	Fe [wt. %]	Min. length [μm]	Max. length [μm]	Average length [μm]	After T6
A	0.123	10.49	52.47	30.04	↓ 51 %
A^{T6}	0.123	3.41	47.96	14.64	
B	0.454	12.06	202.46	59.77	↓ 37 %
B^{T6}	0.454	15.26	117.41	37.56	
C	0,679	9.76	161.48	46.27	↓ 21 %
C^{T6}	0.679	6.57	155.32	36.25	
D	1.209	6.34	141.8	34.42	↓ 15 %
D^{T6}	1.209	5.85	93.25	40.57	

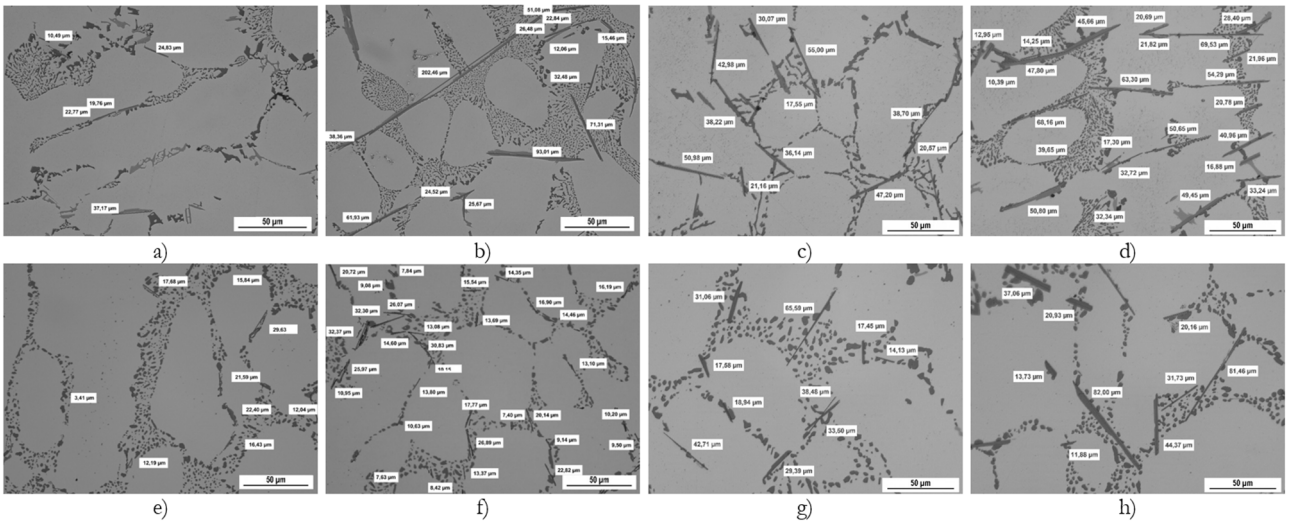

Fig. 3 *Quantitative analysis of Al_5FeSi needles, in as-cast state - a) 0.123 Fe; b) 0.454 Fe, c) 0.679 Fe and d) 1.209 Fe; after T6 - e) 0.123 Fe; f) 0.454 Fe, g) 0.679 Fe and h) 1.209 Fe; etch. H_2SO_4*

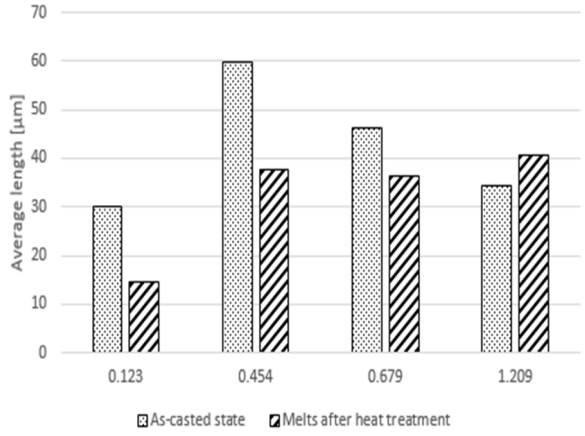

Fig. 4 *Effect of iron content on the average length of Al_5FeSi needles*

3.3 AUDI test

The AUDI test was performed to determine the corrosion behaviour of the examined alloys. After two hours, the samples were removed from the solution, washed, and dried. Then they were weighed and evaluated gravimetrically, i.e., average values of mass changes were calculated. The results of the gravimetric evaluation are displayed in Tab. 3. All alloys recorded weight losses. The AUDI test showed that increasing Fe content leads to a gradual acceleration of corrosion attack. Weight losses grew exponentially with increasing Fe content. This was also the case in alloys without heat treatment as well as after heat treatment. Alloy D (1.209 % Fe) exhibited the worst corrosion resistance, either with or without heat treatment. However, heat treatment does not significantly increase the corrosion resistance of alloys.

Tab. 3 *The results of weight changes after the AUDI Test*

Sample	A	A^{T6}	B	B^{T6}	C	C^{T6}	D	D^{T6}
Weight loss	-0.00768	-0.04197	-0.13040	-0.14266	-0.17596	-0.23626	-0.27205	-0.26296

The macroscopic observation of the surface of the samples is documented in Fig. 5. Macrographs show that all samples were attacked by pitting corrosion. Increasing the Fe content leads to the formation of significantly larger and deeper corrosion pits. The greatest corrosion attack was observed in samples C and D, i.e., in alloys with Fe content greater than 0.679, regardless of the condition of the samples (without heat treatment or after T6). No corrosion products were observed on the surface of the samples.

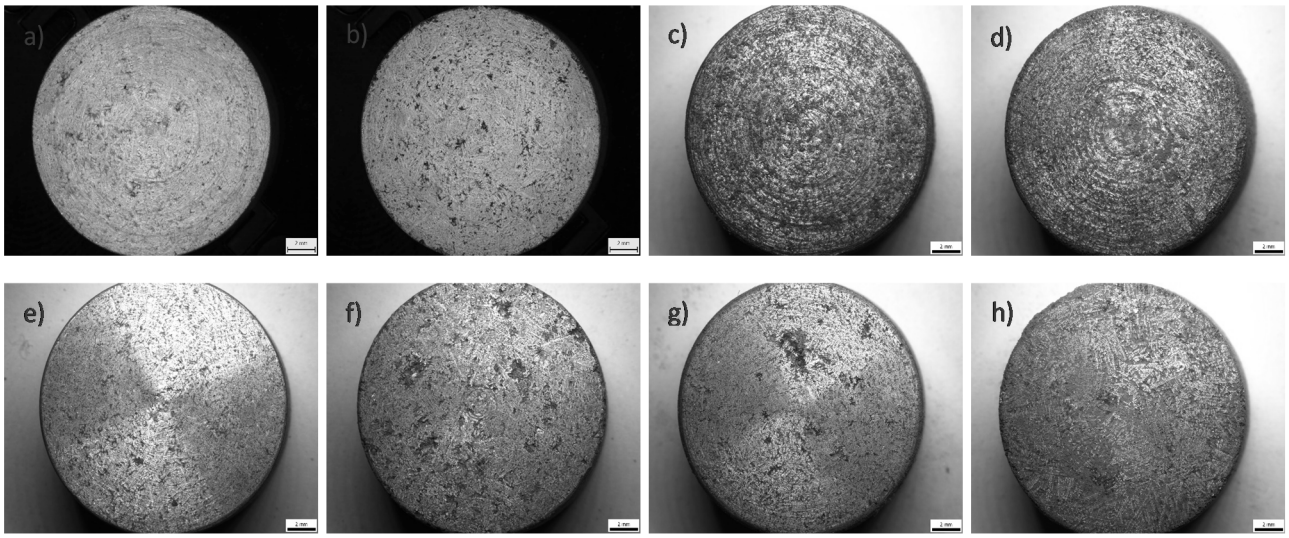

Fig. 5 *Corrosion characteristics of the tested alloys after the AUDI test: in as-cast state - a) 0.123 Fe; b) 0.454 Fe, c) 0.679 Fe and d) 1.209 Fe; after T6: e) 0.123 Fe; f) 0.454 Fe, g) 0.679 Fe and h) 1.209 Fe*

Metallographic analysis of the AlSi7Mg0.3 alloy (cross-section through the samples) confirmed (Fig. 6) that the beginning of pitting corrosion was observed only on the surface of the samples. A preferential attack through the eutectic regions can be observed. It can be concluded that the critical nucleation sites of the corrosion attack are the Al_5FeSi/silicon needle-like phase interfaces, while the primary α-matrix remains unaffected. In the eutectic, corrosion occurs mostly around silicon particles and Fe-phase. Fe and Si are cathodic concerning aluminium and can therefore form a micro galvanic couple together. Therefore, the silicon and Al_5FeSi needle particles act as local cathodes concerning the eutectic phase of aluminium, forming a local galvanic cell, and leading to pitting corrosion [26]. If the galvanic coupling is the main cause of the corrosion, the area ratio between the noble and less noble phases can be one of the key parameters to determine the severity of corrosion [27].

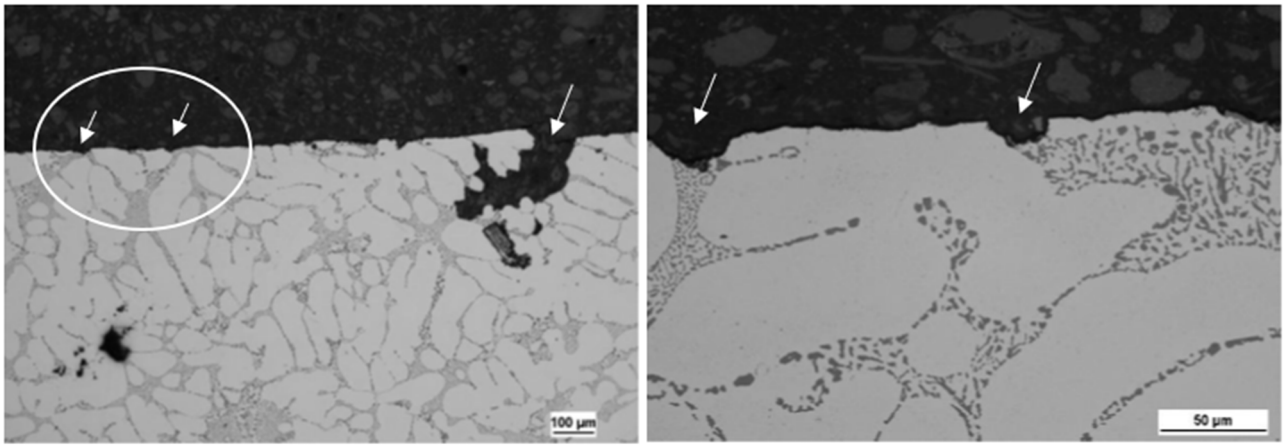

Fig. 6 *Microstructure of alloy with 0.454 Fe (cross-section through the sample): a) surface corrosion attack, b) detail of pits, etch. H_2SO_4*

4 Conclusion

The analysis focused on the influence of increased Fe content on microstructure and corrosion resistance in secondary AlSi7Mg0.3 cast aluminium alloys in the as-cast state and after heat treatment T6. Based on the experimental results the following conclusions can be stated:

- The microstructure of investigated AlSi7Mg0.3 alloy consists of α-phase, eutectic, and intermetallic phases as needle-like Al_5FeSi Fe-phase, and Mg_2Si. The higher Fe content in chemical composition leads to an increased amount of Al_5FeSi intermetallic phases in the microstructure.
- Quantitative analysis shows that a higher Fe content causes an increase in the length of the Fe needle-like phases; however, after the so-called critical iron content is exceeded (alloys C and D), the average length of the needle-like Al_5FeSi phases does not increase any further.
- Heat treatment T6 causes a reduction in the length of the needle phases, the reduction ranging from 51 to 15 %.
- A rapid corrosion test (AUDI test) was used to test the corrosion resistance. This corrosion test proves that increasing Fe content in alloys leads to a gradual acceleration of corrosion attack. As the Fe content increases, the weight of the samples increases exponentially, both in the samples with and without heat treatment.
- Pitting corrosion was observed on the surface of the samples starting at the eutectic. Critical nucleation sites of corrosion attack are the Al_5FeSi/silicon needle-like phase interfaces.

Acknowledgements

The research was supported by Scientific Grand Agency of Ministry of Education of Slovak Republic and Slovak Academy of Sciences, VEGA 01/0398/19, KEGA 016ŽU-4/2020, project to support young researchers at UNIZA, ID project 12715 (Kucharikova) and project 313011ASY4 "Strategic implementation of additive technologies to strengthen the intervention capacities of emergencies caused by the COVID-19 pandemic".

References

[1] *Primary and secondary aluminum*. Clinton Aluminum, 2021. https://www.clintonaluminum.com/primary-and-secondary-aluminum/

[2] TULER, F. R., SCOTT-TAGGART, R. (2001). Aluminum. *Encyclopedia of Materials: Science and Technology*, pp. 97 - 100

[3] *EAA_recycling brochure*: RECYCLING ALUMINIUM A PATHWAY TO A SUSTAINABLE ECONOMY (2015), https://european-aluminium.eu/resource-hub/recycling-aluminium-a-pathway-to-a-sustainable-economy/

[4] KUCHARIKOVÁ, L., TILLOVÁ, E., BOKŮVKA, O. (2016). Recycling and properties of recycled aluminium alloys used in the transportation industry. In: *Transport Problems*, vol. 11, No. 2, pp. 117 - 122

[5] HANZA, S., et al. (2021). Corrosion investigation of Al-Si casting alloys in 0.6 M NaCl solution. In*: Engineering Review*, Vol. 41, No. 3, pp. 115 - 123

[6] SUKIMAN, N. L., et al. (2012). Durability and Corrosion of Aluminium and Its Alloys: Overview, Property Space, Techniques and Developments. In: Ahmad Z, (ed.), Aluminium Alloys – New Trends in Fabrication and Applications. IntechOpen. London. pp. 47 - 97. ISBN 978-953-51-0861-0

[7] HADZIMA, B., LIPTÁKOVÁ, T. (2008). Základy elektrochemickej korózie kovov. Žilinská univerzita v Žiline: EDIS, ISBN 978-80-8070-876-4

[8] DOBKOWSKA, A., et al. (2020). The Comparison of the Microstructure and Corrosion Resistance of Sand Cast Aluminum Alloys. In: *Archives of Metallurgy and Materials*. Vol. 61, No. 1, pp. 209 - 212. ISSN 1733-3490

[9] SVOBODOVA, J., LUNAK, M., LATTNER, M. (2019). Analysis of the Increased Iron Content on the Corrosion Resistance of the AlSi7Mg0.3 Alloy Casting. In: *Manufacturing Technology*, Vol. 19, No. 6, pp. 1041 - 1046

[10] SHOUXUN, J., WENCHAO, Y., et. al. (2013). Effect of iron on the microstructure and mechanical property of Al–Mg–Si–Mn and Al–Mg–Si diecast alloys. In: *Materials Science and Engineering: A,* Vol. 564, pp. 130 - 139

[11] PODPROCKÁ, D., BOLIBRUCHOVÁ, D. (2018). The Role of Manganese in the Alloy Based on Al-Si-Mg with Higher Iron Content. In: *Manufacturing Technology*, Vol. 18, No. 4, pp. 650 - 654. ISSN 1213-2489

[12] RANA, R. S., PUROHIT, R., DAS, S. (2012). Reviews on the Influences of Alloying elements on the Microstructure and Mechanical Properties of Aluminum Alloys and Aluminum Alloy Composites. In: *International Journal of Scientific and Research Publications*, Vol. 2, No. 6, pp 1 - 7

[13] EXCALERA-LOZANO, R., et al. (2010). The Role of Mg2Si in the Corrosion Behavior of Al-Si-Mg Alloys for Pressureless Infiltration. In: *The Open Corrosion Journal,* Vol. 3. No. 1, pp 73 - 79. ISSN: 1876-5033

[14] TAYLOR, J. A. (2004). The effect of iron in Al-Si casting alloys. In: *35th Australian Foundry Institute National Conference.* Adelaide. 148 - 157

[15] KUCHARIKOVÁ, L., et al. (2018). Role of Chemical Composition in Corrosion of Aluminum Alloys. In: *Materials,* Vol. 8, No. 8, pp. 1 - 13. ISSN 2075-4701

[16] ABBAS, M. K. (2016). Effect of Magnesium Addition on Corrosion Resistance of Aluminum -17%Silicon Alloy. In: *Al-Khwarizmi Engineering Journal*, Vol 12, No. 4, pp. 50 - 58

[17] EBHOTA, W.S., TIEN-CHIEN, J. (2018). Intermetallics Formation and Their Effect on Mechanical Properties of Al-Si-X Alloys. In: *Intermetallic Compounds - Formation and Applications.* London: IntechOpen. ISBN 978-1-83881-298-0

[18] KUSMIERCZAK, S., HREN, I. (2019). Influence of AlSi7Mg0.3 Alloy Modification on Corrosion Behaviour in the Salt Environment. In: *Manufacturing Technology,* Vol. 19, No. 5, pp. 802 - 806. ISSN: 1213-2489

[19] FOUSOVA, M., et al. (2019). Corrosion of 3D-Printed AlSi9Cu3Fe Alloy. In: *Manufacturing Technology,* Vol. 19, No. 1, pp. 29 - 36. ISSN 1213-2489

[20] PADMANABAN, D., KURIEN, G. (2012). Silumins: The Automotive Alloys. In: *Advanced Materials and Processes.* Vol. 170, No. 3, pp. 28 - 30. ISSN 0882-7958

[21] ZHU, L., et al. (2018). Light-weighting in aerospace component and system design. In: *Propulsion and Power Research.* Vol. 7, No. 2, pp. 103 - 119. ISSN 2212-540X

[22] ROBLES-HERNANDEZ, F. C., et al. (2017). *Al-Si Alloys - Automotive, Aeronautical, and Aerospace Applications*. Springer, Cham. ISBN 978-3-319-58379-2

[23] KUČERA, V., VOJTĚCH, D. (2017). Influence of heat treatment on corrosion behaviour and mechanical properties of the AA 7075 alloy. In: *Manufacturing Technology.* Vol. 17, No. 5, pp. 747 - 752. ISSN 1213-2489

[24] VANKO, B., STANČEK, L. (2012). Utilization of heat treatment aimed to spheroidization of eutectic silicon for silumin castings produced by squeeze casting. In: *Archives of foundry engineering.* Vol. 12, Iss. 1, pp. 111 - 114. ISSN 1897-3310

[25] STANČEK, L., VANKO, B., BATYŠEV, A. I. (2014). Structure and properties of silumin castings solidified under pressure after heat treatment. In: *Metal Science and Heat Treatment*, vol. 56, No. 3-4, pp. 197 - 202

[26] BERLANGA-LABARI, C.; BIEZMA-MORALEDA, M. V.; RIVERO, P. J. (2020). Corrosion of Cast Aluminum Alloys: A Review. In: *Metals*, 10, 1384

[27] TAHAMTAN, S., BOOSTANI, A. F. (2009). Quantitative analysis of pitting corrosion behavior of thixoformed A356 alloy in chloride medium using electrochemical techniques. In: *Materials and Design*, 30, pp. 2483 - 2489